Biomedical Signal Processing and Control 31 (2017) 569–575

Contents lists available at ScienceDirect

Biomedical Signal Processing and Control

journal homepage: www.elsevier.com/locate/bspc

Association between three-dimensional vessel geometry and the presence of atherosclerotic plaques in the left anterior descending coronary artery of high-risk patients

C.A. Bulant[a,b,*], P.J. Blanco[a,b], A. Clausse[c], A.N. Assunção Jr.[d], T.P. Lima[d], L.F.R. Ávila[d], R.A. Feijóo[a,b], P.A. Lemos[d]

[a] National Laboratory for Scientific Computing, LNCC/MCTI, Av. Getúlio Vargas 333, Quitandinha, 25651-075 Petrópolis, Brazil
[b] National Institute of Science and Technology in Medicine Assisted by Scientific Computing, INCT-MACC, Petrópolis, Brazil
[c] CNEA-CONICET and National University of Central Buenos Aires, 7000 Tandil, Argentina
[d] Heart Institute, University of São Paulo Medical School, INCOR-FM-USP, Av. Dr. Eneas de Carvalho Aguiar, 44, 3rd Floor, São Paulo-SP 05403-000, Brazil

ARTICLE INFO

Article history:
Received 24 June 2016
Received in revised form 24 August 2016
Accepted 29 September 2016
Available online 7 October 2016

Keywords:
Geometric risk factors
Left anterior descending artery
Average distal curvature
Coronary computed tomography angiography
Coronary artery disease

ABSTRACT

Geometrical risk factors for coronary atherosclerosis were proposed in the eighties as a complement to fluid dynamic and biomechanical mechanisms for atherosclerotic genesis and progression. Up to date there are no conclusive results in the subject, although several studies suggest that there is an underlying relation between geometry and disease. Coronary computed tomography angiographies of 48 patients were processed, and the left anterior descending artery (LAD) of each patient was geometrically characterized by computing point-wise curvature. Distal averaging of this feature was used as discriminating variable to identify healthy and diseased arteries. Standard statistical analysis was performed and a binary classifier was used to assess the discriminating capability of the so called average distal curvature ($\bar{\kappa}_d$). A significant difference between the distribution of $\bar{\kappa}_d$ in healthy and diseased LADs was found ($p < 0.01$). Performance of the classifier for a cut-off value of $\bar{\kappa}_d = 0.0537\,\mathrm{mm}^{-1}$ in terms of accuracy, sensitivity and specificity is 75%, 70% and 80% respectively. The area under the receiver-operator curve is 0.75. The results presented here support the hypothesis of a significant correlation between low values of average distal curvature and stenotic lesions in LAD arteries.

© 2016 Elsevier Ltd. All rights reserved.

1. Introduction

Coronary artery disease (CAD) is largely known to be one of the leading causes of death worldwide [1]. Over the last decades, several risk factors for CAD have been identified, comprising mainly modifiable and non-modifiable systemic factors, such as cigarette smoking, diabetes mellitus, hypertension, hypercholesterolemia, familial history [2–4], and genetic contribution to susceptibility for CAD [5–9]. It remains controversial, however, whether systemic risk factors can be fully accounted for the burden and presence of CAD in a given individual [10–12], mainly because they do not explain the localization and non-uniformity of atherosclerosis distribution [13,14].

In this context, a number of biomechanical and geometrical features have been described as factors that would potentially modulate the local atherosclerotic process. And such features are not limited to the coronaries arteries. Specifically, the effect of biomechanical predictors are expressed in terms of several indexes, e.g. wall shear stress and oscillatory shear index [15], and have been supported by extensive evidence [16–20]. In turn, geometrical risk factors [21] suggest that the geometric variability of the human vasculature contributes to the development of atherosclerosis. Several clinical observations back up the geometric hypothesis [22–25]. To date, however, the effects of the later factors remain scarcely reported in the literature, and are not used in clinical practice as conventional risk factors.

Previous efforts to associate lesion presence to shape of coronary arteries focused on the right coronary artery (RCA) [26–28]. This can be attributed to a well defined shape classification (namely: C or Σ) made by visual inspection. In turn, the left anterior descending (LAD) artery lacks of an analogous shape

* Corresponding author at: National Laboratory for Scientific Computing, LNCC/MCTI, Av. Getúlio Vargas 333, Quitandinha, 25651-075 Petrópolis, Brazil.
E-mail addresses: bulant@lncc.br (C.A. Bulant), pjblanco@lncc.br (P.J. Blanco), clausse@exa.unicen.edu.ar (A. Clausse), antonildes@usp.br (A.N. Assunção Jr.), thaples@usp.br (T.P. Lima), avila@incor.usp.br (L.F.R. Ávila), feij@lncc.br (R.A. Feijóo), pedro.lemos@incor.usp.br (P.A. Lemos).

http://dx.doi.org/10.1016/j.bspc.2016.09.023
1746-8094/© 2016 Elsevier Ltd. All rights reserved.

descriptor. Although several geometric features can be used in the characterization of arteries [29], vessel curvature has been used to characterized arteries of several arterial structures, including the internal carotid [30], femoral [31] and cerebral arteries [32], among others. Particularly, curvature values for normal coronary arteries have been reported previously [33].

The present study, focuses on the geometric analysis on the left anterior descending (LAD) artery, searching for any statistically significant correlation between the presence of stenosis and the curvature of the artery. In the present context, arterial geometry is not intended to be used as a standalone tool for lesion detection or diagnostic. In turn, we aimed to present a new potential geometric risk factor for CAD in the LAD: the average distal curvature of the vessel.

The remaining of this document is arranged as follows. Section 2 describes the data and presents the concept of the average distal curvature. Section 3 presents the results of the statistical analysis, which are further discussed in Section 4. Final remarks are outlined in Section 5.

2. Materials and methods

The patient sample used in this work is described in Section 2.1. Computed coronary tomography angiography (CCTA) images were analyzed and processed following a methodology described in [29], and summarized in Section 2.2. Specific aspects of the geometrical analysis for arterial structures are presented in Section 2.3.

2.1. Patient sample demographics

The patient sample used in the present work was originally selected to detect heritability of geometric features on coronary arteries [29], and hence the sample consists of sibling pairs. This is a retrospective study including patients who were referred to CCTA between February 2008 and March 2013 at the Heart Institute (InCor), University of São Paulo Medical School, Brazil. The study protocol was approved by the local ethics committee of the center. The sample selection criterion is described in [29]. A total of 48 patients were selected for this study, consisting of 24 pairs of siblings, 14 females and 34 males patients with an average age of 53 ± 13 years old.

The existence of arterial lesions in the arteries was specified by physicians, and the lesions are characterized according to [34] using a tuple of three variables, namely: stenosis grade, tissue type and lesion position. An artery was considered as diseased when a stenotic lesion of any grade, tissue and position was present in the artery. Altogether, 27 patients presented at least one lesion in the LAD artery, and 21 presented a healthy LAD. The spatial frequency of lesions along the LAD artery for the patient sample is as follows: proximal (21), middle (13) and distal (5). For the purpose of the present study, the target discriminating class is the presence of at least one stenosis (disease, D) as opposed to the complete absence of stenosis (healthy, H).

The demographics of these classes are summarized in Table 1, where continuous variables are expressed as means $\pm$ SD. Normality was assessed using Shapiro–Wilk test. Categorical data are described as numbers (percentage). Comparisons of continuous variables were made using Student's t-test or Mann–Whitney U-test for parametric and non-parametric data, respectively, and χ^2 test or Fisher's exact test for categorical ones. All these tests were performed using STATA 11.0 software (StataCorp., Texas, USA). No statistical significant difference between groups was found, except by the fact that, in our sample, patients with a diseased LAD has an increased probability to suffer stenotic lesions in the other major arteries, the right coronary (RCA) or the left circumflex artery (LCx), $p = 0.01$. Furthermore, all patients have at least one of the major CAD systemic risks factors (smoker, hypertension, diabetes or dyslipidemia). Despite the familial relationship present in the data set, it was shown in [29] that the patient sample is representative from the point of view of the anatomical description of the coronary vasculature, i.e. circulation dominance, lumen radius and arterial occurrence.

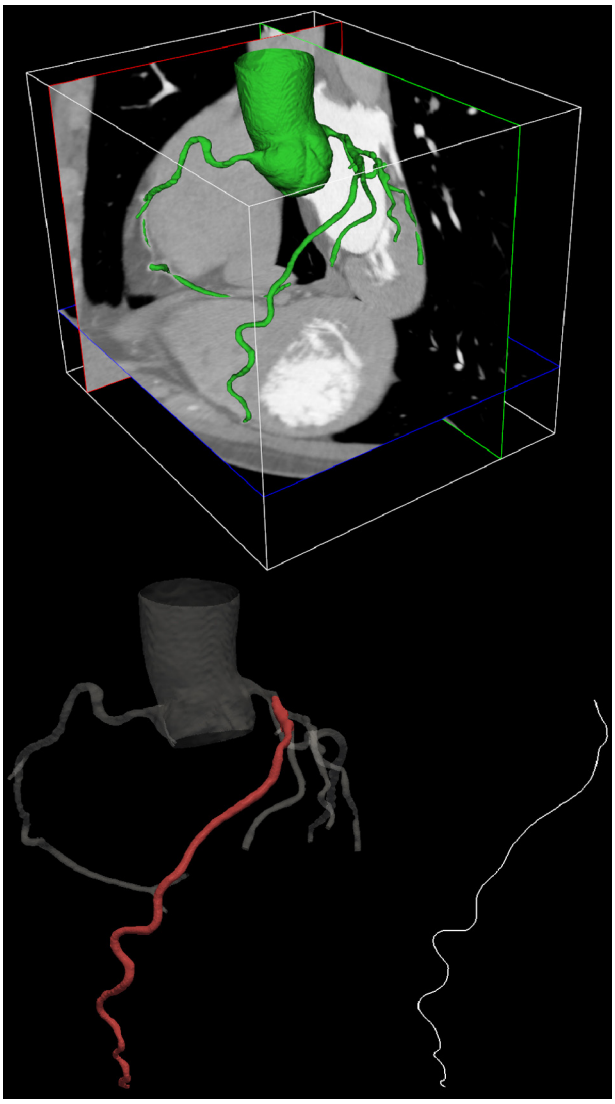

Fig. 1. Illustration of the image processing and centerline construction procedures. Arterial structures segmentation from CCTA (top), mesh post-processing and centerline generation (bottom).

2.2. Data acquisition and processing

The arterial data used in the present study was obtained by means of CCTA. There are also other efficient methods to determine the geometry of arteries, in particular, invasive coronary angiography [37–39], biplane angiography [36], and C-arm scans [40]. However, these other methods may produce distortions of the true curvature of the artery, which is the target of our current interest. Counter to this, noninvasive CCTA images have the advantage of preserving the true spatial disposition of the centerline.

All the medical images were acquired in two devices: a 64-row scanner with a slice thickness of 0.5 mm (Aquilion 64, Toshiba Medical Systems, Japan) and a 320-row scanner system (Aquilion ONE, Toshiba Medical Systems, Japan). All acquisitions were

ECG-triggered prospectively at 75% of the cardiac cycle to keep the lowest possible radiation dose. The acquisition scheme followed standard practice protocols and has been detailed in [29], ensuring patient's heart rate lower to 65 bpm.

Fig. 1 illustrates the image processing pipeline. The arterial lumen is segmented from CCTA images at end-diastole, using a level-set approach [35]; the resulting surface is used for the computation of the arterial path, known as skeleton or centerline [36]. Centerlines are widely accepted models of arterial networks for they exactly retain the arterial topology and most of the geometric characteristics of arteries in a compact and simple structure [29]. In three-dimensional space, centerlines are represented by polylines with point-wise information (e.g. lumen radius), which permits the application of differential geometry analysis to compute, for example, point-wise curvature and torsion.

The geometric models of the arteries consist of three-dimensional polylines with point-wise definition of radius $r(s)$ and curvature $\kappa(s)$, where the absolute arc length of the centerline corresponds to the arc coordinate denoted by s. The curvature is calculated using finite differences over a smoothed polyline, which is constructed by means of a Laplacian filter to eliminate high-frequency noise [32]. This procedure is employed only for the computation of derivatives with respect to the parametric length coordinate.

2.3. Geometrical analysis

The behavior of the point-wise variables $r(s)$ and $\kappa(s)$ for each class, D and H, was explored by averaging the variables over each subsample at each position s, which is discretized in an evenly-spaced scale and linearly interpolated for each patient. Fig. 2 shows the point-wise average for radius and curvature, when normalizing the arc length to the interval [0, 1]. It can be observed that the average curvatures in the distal section and the average radii in the proximal section of the class D are lower than those of the class H. The behavior of the proximal radii is somehow expected since most of the stenoses of the sample are proximal or mid-vessel. Obviously, stenotic lesions are essentially related to the lumen area in the vicinity of the lesion. However, previous evidences have unequivocally documented the diffusiveness of the atherosclerotic process, being frequently present even in seemingly-healthy vessel segments [37]. Therefore, using the vessel radius directly or implicitly to assess the relation to stenosis presence may be questionable.

In order to assess the efficiency of the curvature as a risk indicator of stenosis, the average curvature of each artery was calculated over the distal segment ($\bar{\kappa}_d$). The fraction s_d defining the distal length for averaging is taken as the control parameter. Fig. 3 presents the area under the receiver-operator characteristics curve (AUC) of a classifier method based purely on $\bar{\kappa}_d$ for different values of s_d. In addition, right tailed Mann–Whitney U-Tests were performed to assess statistically significant difference between healthy

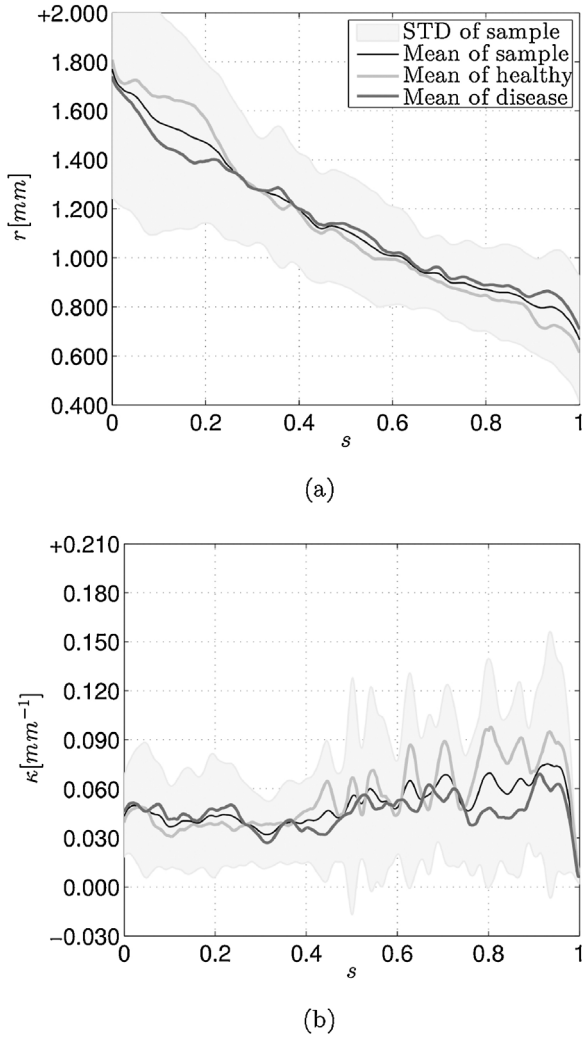

Fig. 2. Comparison of the point-wise averages (curves) and standard deviation (light-gray band) of the entire sample, the healthy and diseased subsamples. Artery lumen radius (a) and vessel curvature (b).

Table 1
Summary of the patient sample demographics. Abbreviations stand for: body mass index (BMI); low-density lipoprotein (LDL); high-density lipoprotein (HDL); myocardial infarction (MI); percutaneous coronary intervention (PCI); coronary artery bypass graft (CABG); left ventricle ejection fraction (LVEF).

Baseline characteristics	All ($n=48$)	Healthy LAD ($n=21$)	Diseased LAD ($n=27$)	p-Value
Age, years ±SD	53.0 ± 13.1	49.3 ± 14.1	55.9 ± 11.8	0.08
Male, n (%)	34 (70.8)	12 (57.1)	22 (81.5)	0.07
BMI, kg/m^2 ±SD	29.0 ± 5.2	28.2 ± 5.7	29.6 ± 4.8	0.11
Hypertension, n (%)	37 (77.1)	14 (66.7)	23 (85.2)	0.17
Diabetes, n (%)	10 (20.6)	2 (9.5)	8 (29.6)	0.15
Dyslipidemia, n (%)	39 (81.2)	16 (76.2)	23 (85.2)	0.47
LDL	123.1 ± 36.9	128.6 ± 40.7	118.7 ± 33.8	0.36
HDL	46.9 ± 10.6	47.3 ± 10.1	46.5 ± 11.0	0.78
Cholesterol	190.4 ± 43.6	196.4 ± 49.9	185.8 ± 38.2	0.41
Smoking, n (%)	14 (29.2)	5 (23.8)	9 (33.3)	0.47
Familiar CAD, n (%)	23 (47.9)	9 (42.9)	14 (51.8)	0.53
Previous MI, n (%)	7 (14.6)	1 (4.8)	6 (22.2)	0.11
Previous PCI, n (%)	5 (10.4)	0 (0)	5 (18.5)	0.06
Previous CABG, n (%)	3 (6.2)	0 (0)	3 (11.1)	0.24
LVEF, % ±SD	63.7 ± 3.7	64.7 ± 3.5	62.9 ± 3.7	0.09
Lesioned RCA/LCx, n (%)	30 (62.5)	9 (42.9)	21 (77.8)	0.01

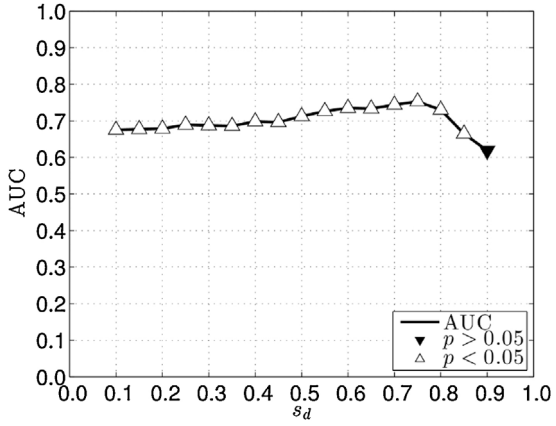

Fig. 3. Area under the receiver-operator curve (AUC) and *U*-Test *p*-values for each partition point s_d.

Table 2
Mann–Whitney *U*-Test and classifier output associated to $s_d = 0.75$. The prevalence of the disease in the population is 56.25%. Abbreviations stand for: area under the receiver operating curve (AUC); positive predictive value (PPV); negative predictive value (NPV).

Statistical summary	
Cut-off value	0.0537 mm^{-1}
Sensitivity	0.7037
Specificity	0.8095
Accuracy	0.75
AUC	0.7531
PPV	0.8261
NPV	0.68
Median H	0.0679 mm^{-1}
Median D	0.0489 mm^{-1}
U	427
p-Value	0.0012
Mean H	0.0771 mm^{-1}
Mean D	0.0479 mm^{-1}

and diseased distributions of $\bar{\kappa}_d$. The results of these tests are presented in Fig. 3. It can be seen that an optimum partition exists when $s_d = 0.75$, that is, averaging over the distal 25% portion of the artery. Section 3 presents the results of the complete analysis for $s_d = 0.75$.

3. Results

Fig. 4a presents a box plot of the distribution of $\bar{\kappa}_d$ for healthy and diseased LADs. Patients in the H class scored higher values (in average) than the D class ($p < 0.01$), implying that diseased vessels have, in average, less curved shape. Fig. 4b shows statistical measures of the performance of the classifier as a function of the discriminating threshold of $\bar{\kappa}_d$. It was found that using a threshold $\bar{\kappa}_d = 0.0537\,\text{mm}^{-1}$ maximizes the accuracy, sensitivity and specificity of the classifier. The associated receiver operator curve is given in Fig. 4c. The optimal AUC score is 0.75. Table 2 details the classifier output and the right tailed *U*-Test used to determine if the mean value of $\bar{\kappa}_d$ was significantly higher in the H class, all using $s_d = 0.75$.

Fig. 5 presents the centerlines of healthy and diseased LADs, and illustrates the difference between them. It can be qualitatively appreciated by visual inspection that the diseased arteries seem to be more straight than healthy ones.

The patient sample used in the present work is composed of siblings. Therefore, some standard test for heritability can be performed. When using the sibling condition (healthy or diseased LAD) as a boolean phenotype, it was found: (i) a high probability that a patient has a lesion given that his sibling has a lesion, given by the probandwise ratio [38] (PBWR = 74%); (ii) the risk ratio or relative risk (RR) is statistically significant RR = 2.2 (with CI = [1.2, 4.2]); (iii) the odds ratio (OR) also scored a significant value OR = 5.7 (with

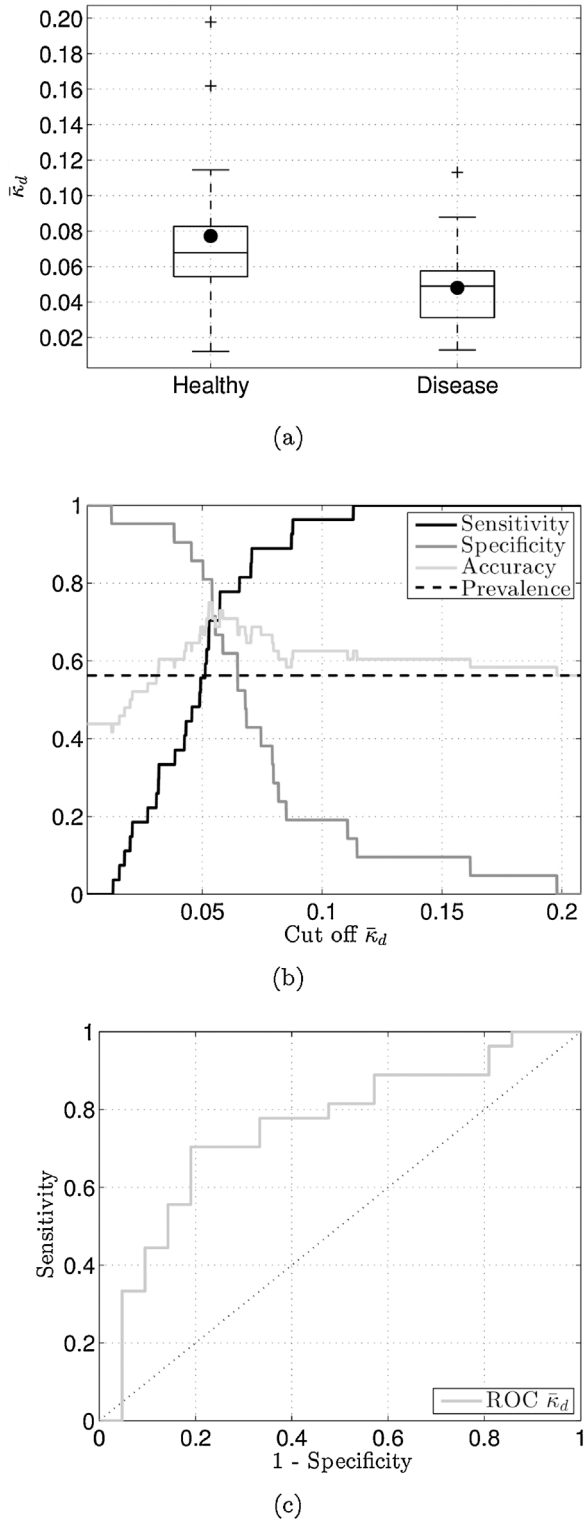

Fig. 4. Panel (a) shows the box plot for $\bar{\kappa}_d$ distribution among healthy and diseased LADs. Patients in the H class scored higher values (in mean) than the D class ($p < 0.01$). Panel (b) presents the performance of the classifier for a range of the $\bar{\kappa}_d$ cut-off value. Panel (c) shows the associated receiver-operator curve. All data correspond to a partition point $s_d = 0.75$.

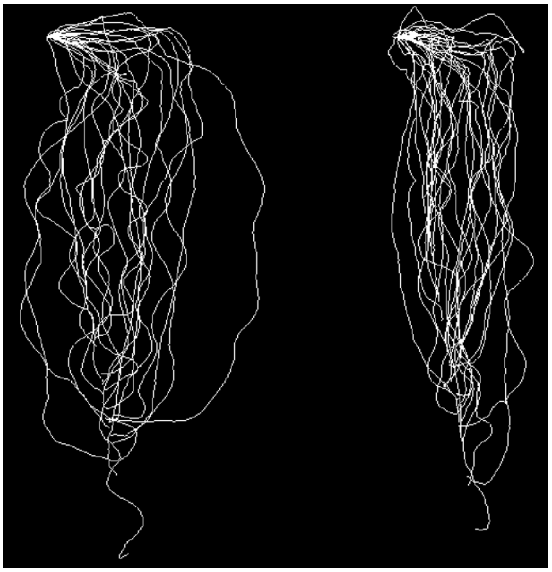

Fig. 5. Illustration of the entire patient sample data. Healthy LADs centerlines are over the left, and diseased over the right.

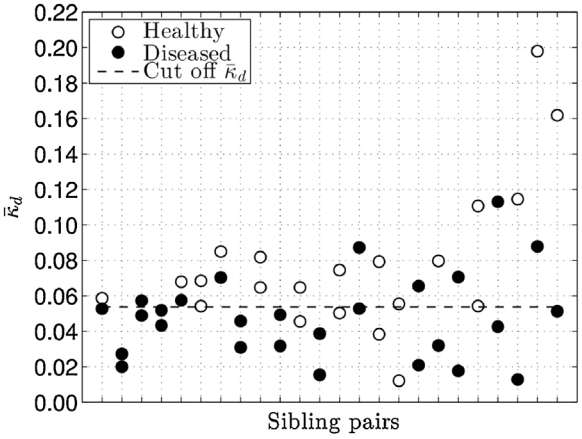

Fig. 6. Scatter plot of average distal curvature ($s_d = 0.75$) per sibling pairs.

CI = [1.6, 20.0]), satisfying the credibility criterion [39] (with a critical odds ratio COR = 3.6).

In turn, the average distal curvature ($\bar{\kappa}_d$), when used as phenotype, yielded no statistically significant outcomes for the Pearson's correlation coefficient (ρ), nor the interclass correlation coefficient (ICC). Furthermore, if the cut-off value ($0.0537\,\mathrm{mm}^{-1}$) is used to dichotomize the $\bar{\kappa}_d$ into a binary phenotype, none of the aforementioned indexes (PBWR, RR and OR) scored significant values.

Fig. 6 presents a scatter plot of $\bar{\kappa}_d$ for each pair of siblings. Healthy and diseased LADs are represented with empty and filled circles respectively, the classifier cut-off value is also displayed. The lack of a strong heritability of the average distal curvature as a standalone geometric descriptor suggests that this feature may be an independent predictor for CAD.

For the sake of completeness, Table 3 presents statistics over the lesioned arteries subsamples, see [34] for details on the lesion characterization. Note that for each subclass of D, the mean $\bar{\kappa}_d$ is smaller than the mean of the *H*. Due to the small size of subclasses, no further statistical tests were performed.

Table 3
Statistical description of lesions of the LAD. Lesions are characterized according to [34].

Lesion characteristic	*n* (%)	$\bar{\kappa}_d$, mean ± SD
Stenosis grade		
Minimal	6 (15.4)	0.0427 ± 0.0212
Mild	22 (56.4)	0.0499 ± 0.0248
Moderate	7 (17.9)	0.0545 ± 0.0269
Severe	4 (10.3)	0.0458 ± 0.0204
Position		
Proximal	21 (53.8)	0.0477 ± 0.0247
Middle	13 (33.4)	0.0546 ± 0.0226
Distal	5 (12.8)	0.0551 ± 0.0215
Tissue type		
Soft tissue	4 (10.3)	0.0567 ± 0.0290
Calcification	18 (46.1)	0.0480 ± 0.0242
Mixed	17 (43.6)	0.0497 ± 0.0224
Lesioned	27	0.0479 ± 0.0241
Healthy	21	0.0771 ± 0.0413

4. Discussion

Curvature patterns in LAD arteries have been characterized before by Zhu et al. [33] using a sample of healthy LADs. In that study, the distal section of the artery is defined as the fraction of the artery from the second diagonal branch to the arterial end, which in most cases brackets distal segments longer than the last 25% of the artery length. Nevertheless, the reported median distal curvature of healthy LADs is $0.057\,\mathrm{mm}^{-1}$, which is within the range of healthy arteries found in the present study, i.e. $\bar{\kappa}_d > 0.0537\,\mathrm{mm}^{-1}$.

Although the statement that LADs with straighter distal segments are more prone to display stenotic lesion appears counterintuitive at first sight, similar results have been previously reported for the right coronary artery (RCA). Dvir et al. [27] reported that C-shaped RCAs are associated with more atherosclerotic disease than sigma-shaped RCAs. Demirgab et al. [28] showed that C-shape is an independent predictor of significant CAD. Arbel et al. [40] reported that flow-mediated endothelium-dependent dilation in the brachial artery is significantly higher in sigma-shaped compared to C-shaped, suggesting a potential mechanism whereby C-shaped RCA are susceptible to atherosclerosis. In this context, it can be conjectured the existence of a global anatomical behavior of the coronary tree associated to plaque formation. The results of the present study support this conjecture. Following this rationale, we have recently shown [29] that curvature derived features in the main coronary arteries are positively correlated.

On the other hand, considering that the present study was performed over a high-risk population, with all patients presenting at least one of the major systemic risk factor (smoker, hypertension, diabetes and/or dyslipidemia), one might hypothesize that high distal curvatures may represent a potential physiological protective mechanism against plaque formation in LAD arteries.

It is also possible that straightness of the distal LAD arteries is a consequence, not a cause, of the atherosclerotic process. In this scenario, the ultimate morphology of a coronary vessel would be shaped by the disease (as hypothesized in [40] for the RCA), and accordingly, atherosclerosis would cause arteries to remodel geometry over time. To the best of our knowledge, no study in the literature has documented this trend so far, which calls for further investigation.

The association of grade, location and tissue of atherosclerotic lesions to the arterial curvature is out of the scope of this work. Such association will be matter of research with larger patient samples.

In spite of the increasing evidence associating CAD to geometric characteristics of the coronary arteries [21–24,27,28,40], the shape of the coronary arteries is not used as a conventional risk factor in

clinical practice, i.e. is not used to explain CAD. However, it should be mentioned that not all geometric characteristics correlate significantly with CAD. The characterization of coronary trees by means of allometric laws relating arterial length, diameter and volume, proposed in [41], does not yield conclusive results in this respect. Counter to that, the present study suggests that there is a correlation between coronary plaques and shape of the LAD. The main limitation of the present results is the modest number of patients and the obvious selection bias of the study population, due the fact that they are siblings. Nevertheless, it was mentioned above, and shown in [29], that our population is a representative set of patients, which reflects several coronary anatomy statistical data.

5. Final comments

This study has shown a significant geometric difference between healthy and diseased LADs. LADs with atherosclerotic lesions feature smaller distal curvatures. Whether straightness of distal portion of the LAD is a geometrical risk factor or a consequence of atherosclerosis proliferation is subject of further investigation.

Conflict of interest statement

We would like to disclose that we do not have any financial and personal relationship with other people or organizations that could inappropriately influence or bias this work.

Acknowledgements

This work was partially supported by the Brazilian agencies CNPq and FAPERJ. The support of these agencies is gratefully acknowledged.

References

[1] G.A. Roth, M.H. Forouzanfar, A.E. Moran, R. Barber, G. Nguyen, V.L. Feigin, M. Naghavi, G.A. Mensah, C.J. Murray, Demographic and epidemiologic drivers of global cardiovascular mortality, N. Engl. J. Med. 372 (14) (2015) 1333–1341.
[2] J. Slack, K.A. Evans, The increased risk of death from ischaemic heart disease in first degree relatives of 121 men and 96 women with ischaemic heart disease, J. Med. Genet. 3 (4) (1966) 239–257.
[3] L.B. Jorde, R.R. Williams, Relation between family history of coronary artery disease and coronary risk variables, Am. J. Cardiol. 62 (10) (1988) 708–713.
[4] B.D. Horne, N.J. Camp, J.B. Muhlestein, L.A. Cannon-Albright, Identification of excess clustering of coronary heart diseases among extended pedigrees in a genealogical population database, Am. Heart J. 152 (2) (2006) 305–311.
[5] P. Pajukanta, M. Cargill, L. Viitanen, I. Nuotio, A. Kareinen, M. Perola, J.D. Terwilliger, E. Kempas, M. Daly, H. Lilja, et al., Two loci on chromosomes 2 and X for premature coronary heart disease identified in early- and late-settlement populations of Finland, Am. J. Hum. Genet. 67 (6) (2000) 1481–1493.
[6] N.J. Samani, P. Burton, M. Mangino, S.G. Ball, A.J. Balmforth, J. Barrett, T. Bishop, A. Hall, BHF Family Heart Study Research Group, A genomewide linkage study of 1,933 families affected by premature coronary artery disease: The British Heart Foundation (BHF) Family Heart Study, Am. J. Hum. Genet. 77 (6) (2005) 1011–1020.
[7] M. Farrall, F.R. Green, J.F. Peden, P.G. Olsson, R. Clarke, M.-L. Hellenius, S. Rust, J. Lagercrantz, M.G. Franzosi, H. Schulte, A. Carey, G. Olsson, G. Assmann, G. Tognoni, R. Collins, A. Hamsten, H. Watkins, Genome-wide mapping of susceptibility to coronary artery disease identifies a novel replicated locus on chromosome 17, PLoS Genet. 2 (5) (2006) e72.
[8] N.J. Samani, J. Erdmann, A.S. Hall, C. Hengstenberg, M. Mangino, B. Mayer, R.J. Dixon, T. Meitinger, P. Braund, H.-E. Wichmann, et al., Genomewide association analysis of coronary artery disease, N. Engl. J. Med. 357 (5) (2007) 443–453.
[9] R. McPherson, A. Pertsemlidis, N. Kavaslar, A. Stewart, R. Roberts, D.R. Cox, D.A. Hinds, L.A. Pennacchio, A. Tybjaerg-Hansen, A.R. Folsom, E. Boerwinkle, H.H. Hobbs, J.C. Cohen, A common allele on chromosome 9 associated with coronary heart disease, Science 316 (5830) (2007) 1488–1491.
[10] C.H. Hennekens, Increasing burden of cardiovascular disease current knowledge and future directions for research on risk factors, Circulation 97 (11) (1998) 1095–1102.
[11] P. Magnus, R. Beaglehole, The real contribution of the major risk factors to the coronary epidemics: time to end the only-50% myth, Arch. Intern. Med. 161 (22) (2001) 2657–2660.
[12] J. McGill, C. Henry, C.A. McMahan, S.S. Gidding, Preventing heart disease in the 21st century: implications of the pathobiological determinants of atherosclerosis in youth (PDAY) study, Circulation 117 (9) (2008) 1216–1227, PMID: 18316498.
[13] D.A. Halon, D. Sapoznikov, B.S. Lewis, M.S. Gotsman, Localization of lesions in the coronary circulation, Am. J. Cardiol. 52 (8) (1983) 921–926.
[14] Y.S. Chatzizisis, G.D. Giannoglou, G.E. Parcharidis, G.E. Louridas, Is left coronary system more susceptible to atherosclerosis than right? A pathophysiological insight, Int. J. Cardiol. 116 (1) (2007) 7–13.
[15] F.B. Gessner, Brief reviews: hemodynamic theories of atherogenesis, Circ. Res. 33 (3) (1973) 259–266.
[16] D.N. Ku, D.P. Giddens, C.K. Zarins, S. Glagov, Pulsatile flow and atherosclerosis in the human carotid bifurcation. Positive correlation between plaque location and low oscillating shear stress, Arterioscler. Thromb. Vasc. Biol. 5 (3) (1985) 293–302.
[17] C.K. Zarins, D.P. Giddens, B.K. Bharadvaj, V.S. Sottiurai, R.F. Mabon, S. Glagov, Carotid bifurcation atherosclerosis. Quantitative correlation of plaque localization with flow velocity profiles and wall shear stress, Circ. Res. 53 (4) (1983) 502–514.
[18] D.P. Giddens, C.K. Zarins, S. Glagov, The role of fluid mechanics in the localization and detection of atherosclerosis, J. Biomech. Eng. 115 (4B) (1993) 588–594.
[19] B.P. Chen, Y.S. Li, Y. Zhao, K.D. Chen, S. Li, J. Lao, S. Yuan, J.Y. Shyy, S. Chien, DNA microarray analysis of gene expression in endothelial cells in response to 24-h shear stress, Physiol. Genomics 7 (1) (2001) 55–63.
[20] P.F. Davies, D.C. Polacek, C. Shi, B.P. Helmke, The convergence of haemodynamics, genomics, and endothelial structure in studies of the focal origin of atherosclerosis, Biorheology 39 (3) (2002) 299–306.
[21] M.H. Friedman, O.J. Deters, F.F. Mark, C.B. Bargeron, G.M. Hutchins, Arterial geometry affects hemodynamics: a potential risk factor for atherosclerosis, Atherosclerosis 46 (2) (1983) 225–231.
[22] U. Ikeda, M. Kuroki, T. Ejiri, S. Hosoda, T. Yaginuma, Stenotic lesions and the bifurcation angle of coronary arteries in the young, Jpn. Heart J. 32 (5) (1991) 627–633.
[23] M.H. Friedman, P.B. Baker, Z. Ding, B.D. Kuban, Relationship between the geometry and quantitative morphology of the left anterior descending coronary artery, Atherosclerosis 125 (2) (1996) 183–192.
[24] H. Zhu, Relationship between the dynamic geometry and wall thickness of a human coronary artery, Arterioscler. Thromb. Vasc. Biol. 23 (12) (2003) 2260–2265.
[25] T.G. Phan, R.J. Beare, D. Jolley, G. Das, M. Ren, K. Wong, W. Chong, M.D. Sinnott, J.E. Hilton, V. Srikanth, Carotid artery anatomy and geometry as risk factors for carotid atherosclerotic disease, Stroke 43 (6) (2012) 1596–1601.
[26] D. Dvir, R. Kornowski, T. Ben-Gal, M. Berman, B. Vidne, D. Aravot, Relation of amounts of narrowing to the length of the right coronary artery, Am. J. Cardiol. 90 (1) (2002) 46–48.
[27] D. Dvir, R. Kornowski, J. Gurevich, B. Orlov, D. Aravot, Degrees of severe stenoses in sigma-shaped versus C-shaped right coronary arteries, Am. J. Cardiol. 92 (3) (2003) 294–298.
[28] R. Demirbag, R. Yilmaz, Effects of the shape of coronary arteries on the presence, extent, and severity of their disease, Heart Vessels 20 (5) (2005) 224–229.
[29] C.A. Bulant, P.J. Blanco, T.P. Lima, A.N. Assunção, G. Liberato, J.R. Parga, L.F.R. Ávila, A.C. Pereira, R.A. Feijóo, P.A. Lemos, A computational framework to characterize and compare the geometry of coronary networks, Int. J. Numer. Methods Biomed. Eng. (2016), http://dx.doi.org/10.1002/cnm.2800.
[30] L.M. Sangalli, P. Secchi, S. Vantini, A. Veneziani, A case study in exploratory functional data analysis: geometrical features of the internal carotid artery, J. Am. Stat. Assoc. 104 (485) (2009) 37–48.
[31] N.B. Wood, S.Z. Zhao, A. Zambanini, M. Jackson, W. Gedroyc, S.A. Thom, A.D. Hughes, X.Y. Xu, Curvature and tortuosity of the superficial femoral artery: a possible risk factor for peripheral arterial disease, J. Appl. Physiol. (Bethesda, Md.: 1985) 101 (5) (2006) 1412–1418.
[32] M. Piccinelli, A. Veneziani, D.A. Steinman, A. Remuzzi, L. Antiga, A framework for geometric analysis of vascular structures: application to cerebral aneurysms, IEEE Trans. Med. Imaging 28 (8) (2009) 1141–1155.
[33] H. Zhu, Z. Ding, R.N. Piana, T.R. Gehrig, M.H. Friedman, Cataloguing the geometry of the human coronary arteries: a potential tool for predicting risk of coronary artery disease, Int. J. Cardiol. 135 (1) (2009) 43–52.
[34] G.L. Raff, Chair, A. Abidov, S. Achenbach, D.S. Berman, L.M. Boxt, M.J. Budoff, V. Cheng, T. DeFrance, J.C. Hellinger, R.P. Karlsberg, SCCT guidelines for the interpretation and reporting of coronary computed tomographic angiography, J. Cardiovasc. Comput. Tomogr. 3 (2) (2009) 122–136.
[35] L. Antiga, M. Piccinelli, L. Botti, B. Ene-Iordache, A. Remuzzi, D.A. Steinman, An image-based modeling framework for patient-specific computational hemodynamics, Med. Biol. Eng. Comput. 46 (11) (2008) 1097–1112.
[36] L. Antiga, B. Ene-Iordache, A. Remuzzi, Computational geometry for patient-specific reconstruction and meshing of blood vessels from MR and CT angiography, IEEE Trans. Med. Imaging 22 (5) (2003) 674–684.
[37] B. De Bruyne, F. Hersbach, N.H. Pijls, J. Bartunek, J.-W. Bech, G.R. Heyndrickx, K.L. Gould, W. Wijns, Abnormal epicardial coronary resistance in patients

with diffuse atherosclerosis but “normal” coronary angiography, Circulation 104 (20) (2001) 2401–2406.
[38] M. McGue, When assessing twin concordance, use the probandwise not the pairwise rate, Schizophr. Bull. 18 (2) (1992) 171–176.
[39] R.A.J. Matthews, Methods for assessing the credibility of clinical trial outcomes, Drug Inf. J. 35 (4) (2001) 1469–1478.
[40] Y. Arbel, D. Dvir, M.S. Feinberg, R. Beigel, M. Shechter, The association between right coronary artery morphology and endothelial function, Int. J. Cardiol. 115 (1) (2007) 19–23.
[41] D. Craiem, M.E. Casciaro, S. Graf, E.P. Gurfinkel, R.L. Armentano, Non-invasive assessment of allometric scaling laws in the human coronary tree, Artery Res. 5 (1) (2011) 15–23.